


Two-photon-exchange effect in $ep \rightarrow en\pi^+$ at small $-t$ with the hadronic model and dispersion relation approach

Qian-Qian Guo and Hai-Qing Zhou ^{*}*School of Physics, Southeast University, NanJing 211189, China*

(Received 30 March 2022; revised 30 May 2022; accepted 6 July 2022; published 15 July 2022)

In this paper, the two-photon-exchange (TPE) effect in $ep \rightarrow en\pi^+$ at small $-t$ is discussed. In the previous work, the TPE contribution with one π intermediate state is estimated numerically within a hadronic model under the pion-dominance approximation. Here we extend the discussion to include one ρ intermediate state. The TPE contribution can be described by one scalar function in the limit $m_e \rightarrow 0$, the dispersion relation (DR) satisfied by this scalar function is analyzed. The analytic expressions for the imaginary parts of the TPE contributions from one π or one ρ intermediate state are given within the hadronic model. Combining these analytic expressions and the DR, the corresponding real parts of the TPE contributions can be estimated easily at any available region. This can help the further experimental analysis to include the TPE contributions in a convenient way. The numeric results show that the TPE correction with one ρ intermediate state is much smaller than that with one π intermediate state in the current energy region. These results suggest that the TPE contribution with an elastic state is the main TPE contribution in $ep \rightarrow en\pi^+$ at small $-t$.

DOI: [10.1103/PhysRevC.106.015203](https://doi.org/10.1103/PhysRevC.106.015203)

I. INTRODUCTION

The two-photon-exchange (TPE) effect plays an important role to extract the electromagnetic (EM) form factors (FFs) of the proton from the unpolarized ep scattering and has been widely studied by many theoretical methods, such as the hadronic model [1], the generalized parton distributions method [2], perturbative QCD calculation [3], dispersion relation (DR) approach [4,5], soft collinear effective theory method [6], chiral perturbative theory (ChpT) [7], and phenomenological parametrization [8]. Recently many experimental measurements were developed to test these theoretical estimations and to deepen our understanding on the TPE contribution [9–12].

Comparing with the proton case, the discussions on how to extract the EM FF of π precisely are relatively few. Experimentally, the EM form factor of π is usually extracted via the process $ep \rightarrow en\pi^+$ [13–17]. Theoretically, such extraction of the pion's FF is much more complex than that of the proton's FFs via the elastic ep scattering. The corresponding theoretical analysis on the experimental data sets should be performed more carefully. Up to now, the discussions on the TPE effect in $ep \rightarrow en\pi^+$ are limited [18,19]. In the previous work [19], the TPE contributions with an elastic intermediate

state are discussed, and in this paper we extend the discussion to include one ρ meson intermediate state. Furthermore, the DR for the TPE contributions and the analytic expressions for the imaginary parts are both given.

We organize the paper as follows. In Sec. II we describe the basic frame of our discussion under the pion-dominance approximation, in Sec. III we show some analytic properties of the TPE contributions and the DR relation they satisfied. In Sec. IV we present some numerical results for the TPE corrections and give our conclusion.

II. BASIC FRAME FOR THE TPE CONTRIBUTIONS

IN $ep \rightarrow en\pi^+$

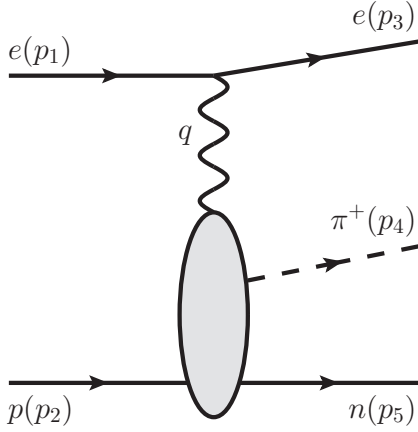
Under the one-photon exchange (OPE) approximation, the process $ep \rightarrow en\pi^+$ can be described by Fig. 1 where we label the momenta of initial electron, initial proton, final electron, final pion, and final neutron as p_{1-5} . For simplicity we define the following five independent Lorentz invariant variables $s \equiv (p_1 + p_2)^2$, $Q^2 \equiv -q^2 \equiv -(p_1 - p_3)^2$, $W \equiv \sqrt{(p_4 + p_5)^2}$, $t \equiv (p_2 - p_5)^2$, and $v = (p_1 + p_3)(2p_4 + p_3 - p_1)$.

When we discuss the TPE effect, the contribution from the corresponding TPE diagram shown in Fig. 2 should be considered.

Physically, the dynamics of the subprocesses $\gamma^*p \rightarrow n\pi^+$ and $\gamma^*\gamma^*p \rightarrow n\pi^+$ are very complex. On the small energy scale, one can expect that the ChpT works well for these two subprocesses. For example, in the leading order of ChpT the Feynman diagrams for $\gamma^*p \rightarrow n\pi^+$ can be described by Fig. 3 where the notations 0 and 1 refer to the power of the momenta in the corresponding vertices. Since the power of the momentum in the pion's propagator is -2 and the power of

*zhouhq@seu.edu.cn

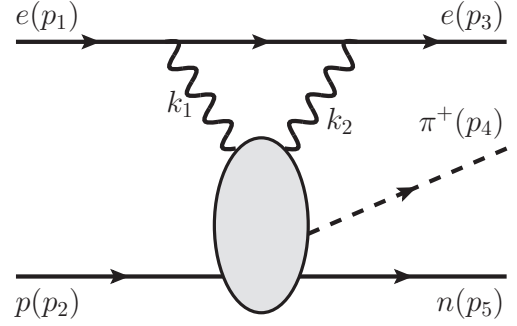
Published by the American Physical Society under the terms of the [Creative Commons Attribution 4.0 International](https://creativecommons.org/licenses/by/4.0/) license. Further distribution of this work must maintain attribution to the author(s) and the published article's title, journal citation, and DOI. Funded by SCOAP³.


 FIG. 1. $ep \rightarrow en\pi^+$ with one-photon exchange.

momentum in the proton's propagator is -1 , the contributions from Figs. 3(a) and 3(b) are on the same order.

When the energy scales $-t$, Q^2 , and W increase, one can expect that ChpT is not valid anymore and the contributions beyond ChpT, such as the diagrams with ρ meson exchange and with N^* intermediate states shown as Fig. 4 should be considered.

When $-t$ is kept small, W is a little far away from the masses of the narrow resonances, and only Q^2 increases, the contribution from one pion-exchange diagrams where only a pion interacts with nucleon is still dominant among all these contributions although ChpT is not valid. The reasons are due to two facts: (1) the mass of pion is close to zero which results in a strong enhancement from the pion propagator, (2) the couplings of γ^*pp , γ^*pN^* decrease much faster than the coupling $\gamma^*\pi\pi$ when Q^2 increases. These properties mean


 FIG. 2. $ep \rightarrow en\pi^+$ with two-photon exchange.

the pion dominance is a good approximation when $t \rightarrow 0$ and W is a little far away from the narrow resonances. This also greatly simplifies the dynamics of the process $\gamma^*\gamma^*p \rightarrow n\pi^+$ in this region. In this paper, we limit our discussion on the TPE contributions under this approximation. In the practical calculation, one can combine the contributions beyond the pion dominance under the OPE approximation and the TPE contributions together since their contributions are independent.

Under the pion-dominance approximation, the corresponding TPE contributions can be described as Figs. 5(a)–5(c) where the contributions from Figs. 6(a)–6(c) are neglected since they are much smaller.

In the previous work [19], the TPE contributions from an elastic state π shown in Fig. 7 are discussed in the region $Q^2 \subseteq [1, 2.45] \text{ GeV}^2$. At higher Q^2 , the similar contributions with one ρ meson intermediate state shown as Fig. 8 maybe gives some considerable contributions.

Taking the Feynman gauge, one has

$$\begin{aligned}
 \mathcal{M}_{1\gamma}^{(a)} &= -i\bar{u}_e(p_3)(-ie\gamma^\mu)u_e(p_1)\bar{u}_n(p_5)\Gamma_5 u_p(p_2)\Gamma^\nu(p_4, p_t)S_\pi(p_t)D_{\mu\nu}(p_1 - p_3), \\
 \mathcal{M}_{2\gamma,\rho}^{(a)} &= -i\bar{\mu}^{2\epsilon} \int \frac{d^4k_1}{(2\pi)^d} [\bar{u}_e(p_3)(-ie\gamma^\nu)S_F(p_1 - k_1)(-ie\gamma^\mu)u_e(p_1)\bar{u}_n(p_5)\Gamma_5 u_p(p_2)]\Gamma^{\omega\lambda}[(p_1 - k_1 - p_3, p_t + k_1) \\
 &\quad \times S_{\lambda\sigma}^V(p_t + k_1)\Gamma^{\nu\sigma}(k_1, -p_t - k_1)]S_\pi(p_t)D_{\eta\omega}(p_1 - k_1 - p_3)D_{\mu\nu}(k_1), \\
 \mathcal{M}_{2\gamma,\rho}^{(b)} &= -i\bar{\mu}^{2\epsilon} \int \frac{d^4k_1}{(2\pi)^d} [\bar{u}_e(p_3)(-ie\gamma^\mu)S_F(p_1 - k_1)(-ie\gamma^\nu)u_e(p_1)\bar{u}_n(p_5)\Gamma_5 u_p(p_2)]\Gamma^{\omega\lambda}(k_1, p_4 - k_1) \\
 &\quad \times S_{\lambda\sigma}^V(p_4 - k_1)\Gamma^{\nu\sigma}(p_1 - k_1 - p_3, k_1 - p_4)]S_\pi(p_t)D_{\mu\nu}(p_1 - k_1 - p_3)D_{\eta\omega}(k_1),
 \end{aligned} \tag{1}$$

with $\bar{\mu}$ as the introduced energy scale, $d = 4 - 2\epsilon$ as the dimension, $p_t = p_3 + p_4 - p_1$, and

$$\begin{aligned}
 S_F(k) &= \frac{i(\not{k} + m_e)}{k^2 - m_e^2 + i\epsilon}, \\
 S_\pi(k) &= \frac{i}{k^2 - m_\pi^2 + i\epsilon}, \\
 S_{\lambda\sigma}^V(k) &= \frac{-i(g_{\lambda\sigma} - \frac{k_\lambda k_\sigma}{k^2})}{k^2 - m_\rho^2 + i\epsilon}, \\
 D_{\mu\nu}(k) &= \frac{-i}{k^2 + i\epsilon}g_{\mu\nu},
 \end{aligned} \tag{2}$$

and

$$\begin{aligned}
 \Gamma^\mu(p_f, p_i) &= ie\{[1 + f(k^2)k^2](p_f + p_i)^\mu \\
 &\quad - f(k^2)(p_f^2 - p_i^2)k^\mu\},
 \end{aligned} \tag{3}$$

$$\Gamma^{\mu\nu}(k_\gamma, k_\rho) = ieg_{\rho\pi\gamma}/m_\rho F_{\gamma\pi\rho}(k_\gamma^2)\epsilon_{\mu\nu\lambda\omega}k_\gamma^\lambda k_\rho^\omega,$$

where $e = -|e|$, $k \equiv p_f - p_i$, $k_{\gamma,\nu}$ are the incoming momenta of the photon and ρ meson, $f(k^2)$ describes the EM form factor of pion which is defined as [20]

$$\begin{aligned}
 \langle p_f | J_\mu(0) | p_i \rangle &\equiv F_{\gamma\pi\pi}(k^2)(p_i + p_f)_\mu, \\
 F_{\gamma\pi\pi}(k^2) &\equiv 1 + k^2 f(k^2),
 \end{aligned} \tag{4}$$

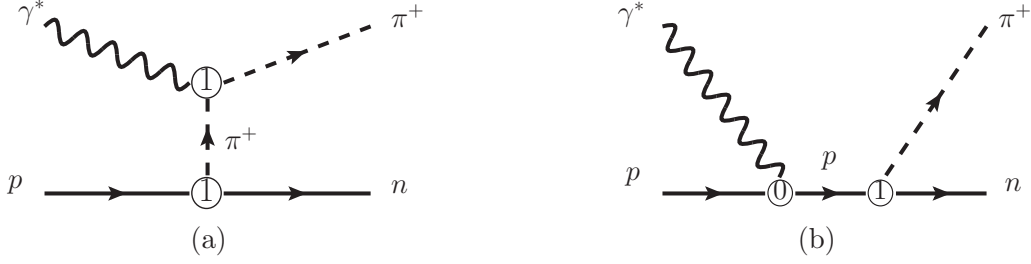


FIG. 3. Diagrams for $\gamma^* p \rightarrow n\pi^+$ in the leading order of ChpT with (a) the pion exchange diagram and (b) the elastic s -channel diagram.

with $J_\mu = \sum e_i \bar{\psi}_i \gamma_\mu \psi_i$, ψ_i as the quark fields, i as the flavor indexes of the quarks, and e_i as the corresponding electric charges of quarks (-1 for the electron). $F_{\gamma\pi\rho}(k_\gamma^2)$ is the transition FF of $\gamma^*\pi \rightarrow \rho$ [21]. The similar expressions $\mathcal{M}_{2\gamma,\pi}^{(a,b,c)}$ corresponding to Figs. 7(a)–7(c) can be found in Ref. [19]. In the practical calculation, one can find that the relative TPE corrections are not dependent on the form of Γ_5 (pseudoscalar form or pseudovector form) since it appears both in the tree diagram and in the TPE diagrams. So we do not present its form here.

Generally, the amplitudes with one-pion exchange can be written as the following simple form:

$$\begin{aligned} \mathcal{M}_{1\gamma} &\equiv \mathcal{M}_{1\gamma}^{(a)} = c_1^{(1\gamma)} \mathcal{M}_1 + c_2^{(1\gamma)} \mathcal{M}_2, \\ \mathcal{M}_{2\gamma,\pi} &\equiv \mathcal{M}_{2\gamma,\pi}^{(a+b+c)} = c_{1,\pi}^{(a+b+c)} \mathcal{M}_1 + c_{2,\pi}^{(a+b+c)} \mathcal{M}_2, \\ \mathcal{M}_{2\gamma,\rho} &\equiv \mathcal{M}_{2\gamma,\rho}^{(a+b)} = c_{1,\rho}^{(a+b)} \mathcal{M}_1 + c_{2,\rho}^{(a+b)} \mathcal{M}_2, \end{aligned} \quad (5)$$

with

$$\begin{aligned} \mathcal{M}_1 &\equiv i\bar{u}(p_3, m_e)(2\not{p}_4 + \not{p}_3 - \not{p}_1)u(p_1, m_e) \\ &\quad \times \bar{u}(p_5, m_n)\Gamma_5 u(p_2, m_p), \\ \mathcal{M}_2 &\equiv i\bar{u}(p_3, m_e)u(p_1, m_e)\bar{u}(p_5, m_n)\Gamma_5 u(p_2, m_p). \end{aligned} \quad (6)$$

The coefficients $c_{1,2}^{(1\gamma)}$ can be easily obtained which are expressed as

$$\begin{aligned} c_1^{(1\gamma)} &= \frac{4\pi\alpha_e F_\pi(q^2)}{Q^2(t - m_\pi^2)}, \\ c_2^{(1\gamma)} &= 0, \end{aligned} \quad (7)$$

with $\alpha_e \equiv e^2/4\pi$.

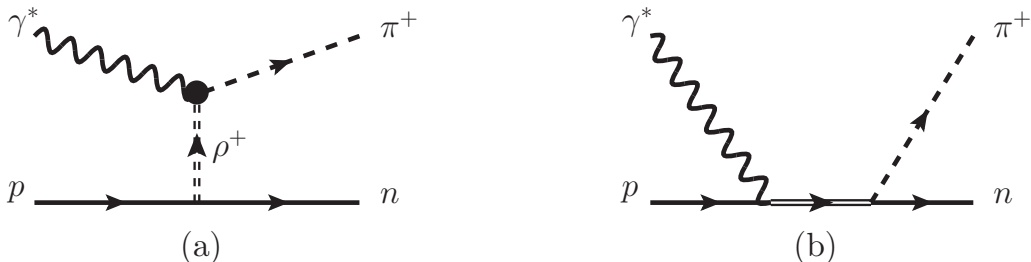


FIG. 4. Examples of diagrams for $\gamma^* p \rightarrow n\pi^+$ beyond ChpT with (a) ρ meson exchange and (b) N^* contribution.

III. SOME ANALYTIC PROPERTIES OF THE TPE CONTRIBUTIONS IN $ep \rightarrow en\pi^+$

A. General properties due to the symmetry

When taking the limit $m_e \rightarrow 0$, the QED interaction will not flip the helicity of the electron. Then one has the following exact property:

$$c_{2,\pi}^{(a+b)}, c_{2,\rho}^{(a+b)} \rightarrow 0. \quad (8)$$

Furthermore, due to the crossing symmetry of the diagram Fig. 7(c), one has

$$c_{1,\pi}^{(c)} = 0.$$

In literature, the approximation $m_e = 0$ is often used before the loop integration since m_e is much smaller than the other scales in the experimental region. In the elastic ep scattering and elastic $e\pi$ scattering cases, one can find that such an approach works well since the full TPE contributions are not dependent on m_e at the leading order of m_e . In $ep \rightarrow en\pi^+$, we find that such an approach is good for $c_{1,\rho}^{(a+b)}$ but not good for $c_{1,\pi}^{(a+b)}$. This is very different from the ep or $e\pi$ cases and beyond the naive estimation. The detailed analytic calculation shows that there is a term, such as $\ln m_e$ in $c_{1,\pi}^{(a+b)}$ when taking $m_e \rightarrow 0$ after the loop calculation. Such a term means that the result by applying Taylor series expansion before the loop integration is different from the result by applying Taylor series expansion after the loop integration. This is natural since the loop integration and the Taylor series expansion are not commuted in some cases. Our numerical results also show such a property and such a logarithm enhancement should be dealt carefully.

To keep this term, in the following calculation we at first take m_e as nonzero to perform loop integration and then expand the results on m_e . The packages FEYNALCALC [22],

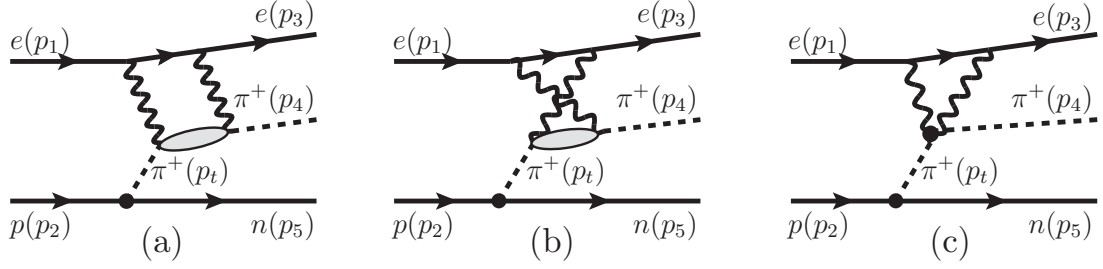


FIG. 5. Diagrams for $ep \rightarrow en\pi^+$ with two-photon exchange under the pion-dominance approximation: (a) is the box diagram, (b) is the crossed-box diagram, and (c) is the contact diagram.

PACKAGE-X V3.00 [23], and LOOPTOOLS [24] are used in the practical calculations.

Under the pion-dominance approximation, although the cross sections are dependent on five variables, but the TPE contributions $c_{1,\pi;1,\rho}^{(a,b)}$ are only dependent on three variables t , Q^2 , and ν . Due to the crossing symmetry, one has the following general relation when Q^2 and t are fixed in the physical region:

$$c_{1,\pi;1,\rho}^{(a)}(\nu^+, Q^2, t) = -c_{1,\pi;1,\rho}^{(b)}(-\nu^+, Q^2, t), \quad (9)$$

where $\nu^+ = \nu + i0^+$.

B. TPE contributions in the pointlike particle case

To show the analytic properties of the TPE contribution in a clear form, at first we take the pointlike interaction as an example. In this case, one has

$$F_{\gamma\pi\pi}^I(k^2) = F_{\gamma\pi\rho}^I(k^2) = 1, \quad (10)$$

where we have used index I to refer to the pointlike interaction. The same index is used for other quantities in the following expressions.

After the loop integration, we find the following analytic properties:

- (1) There are no kinematic poles in $c_{1,\pi;1,\rho}^{I(a,b)}$.
- (2) When t and Q^2 are fixed as physical values, the branch cuts of $c_{1,\pi;1,\rho}^{I(a,b)}$ on ν are shown as Fig. 9.
- (3) The asymptotic behaviors of $c_{1,\pi;1,\rho}^{I(a)}$ are expressed as follows:

$$\begin{aligned} \text{Re}[c_{1,\pi}^{I(a)}(\nu^+, Q^2, t)] &\xrightarrow{\nu \rightarrow \infty} \frac{2\alpha_e^2}{Q^2(m_\pi^2 - t)} \left[\ln^2 \nu - \left(\frac{1}{\tilde{\epsilon}_{\text{IR}}} + \ln \frac{4m_e^2(m_\pi^2 - t)^2 \tilde{\mu}_{\text{IR}}^2}{Q^4} \right) \ln \nu + O(\nu^0) \right], \\ \text{Im}[c_{1,\pi}^{I(a)}(\nu^+, Q^2, t)] &\xrightarrow{\nu \rightarrow \infty} \frac{2\pi\alpha_e^2}{Q^2(m_\pi^2 - t)} \left[-2 \ln \nu + \left(\frac{1}{\tilde{\epsilon}_{\text{IR}}} + \ln \frac{4m_e^2(m_\pi^2 - t)^2 \tilde{\mu}_{\text{IR}}^2}{Q^4} \right) + O(\nu^{-1}) \right], \end{aligned} \quad (11)$$

and

$$\begin{aligned} \text{Re}[c_{1,\rho}^{I(a)}(\nu^+, Q^2, t)] &\xrightarrow{\nu \rightarrow \infty} \frac{\alpha_e^2 \delta_{\gamma\pi\rho}^2}{8m_\rho^2(m_\pi^2 - t)} [2 \ln^2 \nu - (4 \ln Q^2 + 3 + 4 \ln 2) \ln \nu + O(\nu^0)], \\ \text{Im}[c_{1,\rho}^{I(a)}(\nu^+, Q^2, t)] &\xrightarrow{\nu \rightarrow \infty} \frac{\pi\alpha_e^2 \delta_{\gamma\pi\rho}^2}{8m_\rho^2(m_\pi^2 - t)} [-4 \ln \nu + (4 \ln Q^2 + 3 + 4 \ln 2) + O(\nu^{-1})], \end{aligned} \quad (12)$$

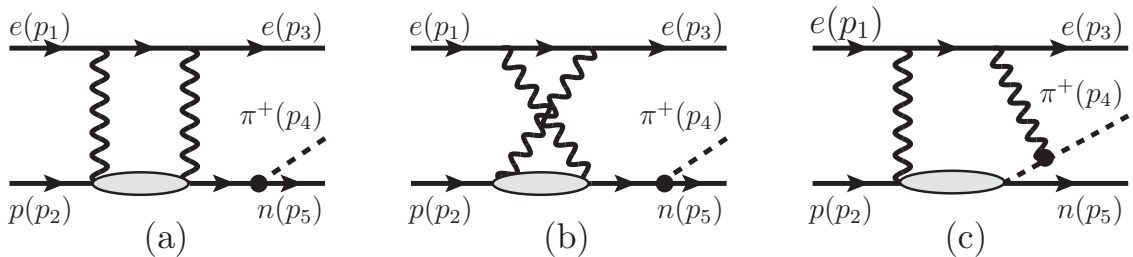


FIG. 6. Diagrams for $ep \rightarrow en\pi^+$ with two-photon exchange beyond the pion-dominance approximation.

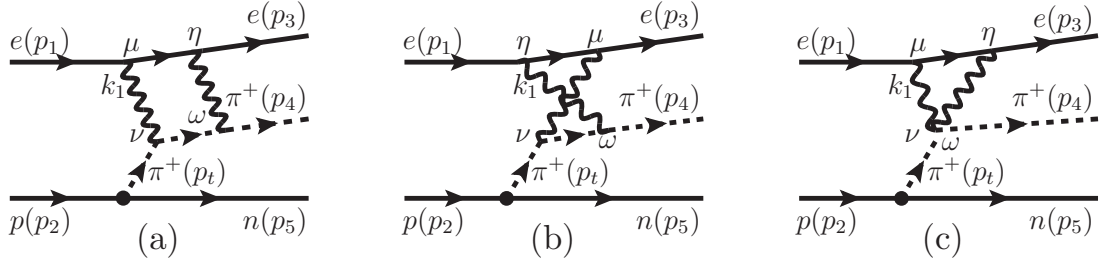


FIG. 7. Diagrams for $ep \rightarrow e\pi^+$ with two-photon exchange and one π meson intermediate state: (a) is the box diagram, (b) is the crossed diagram, and (c) is the contact diagram.

where $\bar{\mu}_{\text{IR}}$ is the IR scale, and

$$\frac{1}{\bar{\epsilon}_{\text{IR}}} = \frac{1}{\epsilon_{\text{IR}}} - \gamma_E + \ln 4\pi.$$

The asymptotical behaviors of $c_{1,\pi;1,\rho}^{1,(b)}$ in the limit $\nu \rightarrow -\infty$ can be obtained easily via Eq. (9).

Based on the properties of the asymptotic behaviors and the position of the branch cut, one can get the once-subtracted DR,

$$\text{Re}[c_{1,\pi;1,\rho}^{1,(a)}(\nu, Q^2, t)] - \text{Re}[c_{1,\pi;1,\rho}^{1,(a)}(\nu_1, Q^2, t)] = \frac{\nu - \nu_1}{\pi} \text{Re} \left[\int_{\nu_{\text{th}}^{(\pi,\rho)}}^{\infty} \frac{\text{Im}[c_{1,\pi;1,\rho}^{1,(a)}(\bar{\nu}^+, Q^2, t)]}{(\bar{\nu} - \nu - i\epsilon)(\bar{\nu} - \nu_1 - i\epsilon)} d\bar{\nu} \right],$$

where $\nu_{\text{th}}^{(\pi)} = m_\pi^2 + 4m_e m_\pi - Q^2 - t$, $\nu_{\text{th}}^{(\rho)} = 2m_\rho^2 - m_\pi^2 + 4m_e m_\rho - Q^2 - t$. Similarly one has

$$\text{Re}[c_{1,\pi;1,\rho}^{1,(b)}(\nu, Q^2, t)] - \text{Re}[c_{1,\pi;1,\rho}^{1,(b)}(\nu_2, Q^2, t)] = \frac{\nu - \nu_2}{\pi} \text{Re} \left[\int_{-\infty}^{-\nu_{\text{th}}^{(\pi,\rho)}} \frac{\text{Im}[c_{1,\pi;1,\rho}^{1,(b)}(\bar{\nu}^+, Q^2, t)]}{(\bar{\nu} - \nu + i\epsilon)(\bar{\nu} - \nu_2 + i\epsilon)} d\bar{\nu} \right].$$

Taking ν_2 as $-\nu_1$ and using the property Eq. (9), one has

$$\begin{aligned} & \text{Re}[c_{1,\pi;1,\rho}^{1,(b)}(\nu, Q^2, t)] + \text{Re}[c_{1,\pi;1,\rho}^{1,(a)}(\nu_1, Q^2, t)] \\ &= \frac{\nu + \nu_1}{\pi} \text{Re} \left[\int_{-\infty}^{-\nu_{\text{th}}^{(\pi,\rho)}} \frac{\text{Im}[c_{1,\pi;1,\rho}^{1,(b)}(\bar{\nu}^+, Q^2, t)]}{(\bar{\nu} - \nu + i\epsilon)(\bar{\nu} + \nu_1 + i\epsilon)} d\bar{\nu} \right] \\ &= -\frac{\nu + \nu_1}{\pi} \text{Re} \left[\int_{-\infty}^{-\nu_{\text{th}}^{(\pi,\rho)}} \frac{\text{Im}[c_{1,\pi;1,\rho}^{1,(a)}(-\bar{\nu}^+, Q^2, t)]}{(\bar{\nu} - \nu + i\epsilon)(\bar{\nu} + \nu_1 + i\epsilon)} d\bar{\nu} \right] \\ &= -\frac{\nu + \nu_1}{\pi} \text{Re} \left[\int_{\nu_{\text{th}}^{(\pi,\rho)}}^{\infty} \frac{\text{Im}[c_{1,\pi;1,\rho}^{1,(a)}(\bar{\nu}^-, Q^2, t)]}{(\bar{\nu} + \nu + i\epsilon)(\bar{\nu} - \nu_1 + i\epsilon)} d\bar{\nu} \right] \end{aligned}$$

$$= \frac{\nu + \nu_1}{\pi} \text{Re} \left[\int_{\nu_{\text{th}}^{(\pi,\rho)}}^{\infty} \frac{\text{Im}[c_{1,\pi;1,\rho}^{1,(a)}(\bar{\nu}^+, Q^2, t)]}{(\bar{\nu} + \nu + i\epsilon)(\bar{\nu} - \nu_1 + i\epsilon)} d\bar{\nu} \right].$$

Combing these two results, finally one gets the unsubtracted dispersion relation,

$$\text{Re}[c_{1,\pi;1,\rho}^{1,(a+b)}(\nu, Q^2, t)] = \frac{2\nu}{\pi} \text{Re} \left[\int_{\nu_{\text{th}}^{(\pi,\rho)}}^{\infty} \frac{\text{Im}[c_{1,\pi;1,\rho}^{1,(a)}(\bar{\nu}^+, Q^2, t)]}{\bar{\nu}^2 - \nu^2 - i\epsilon} d\bar{\nu} \right]. \quad (13)$$

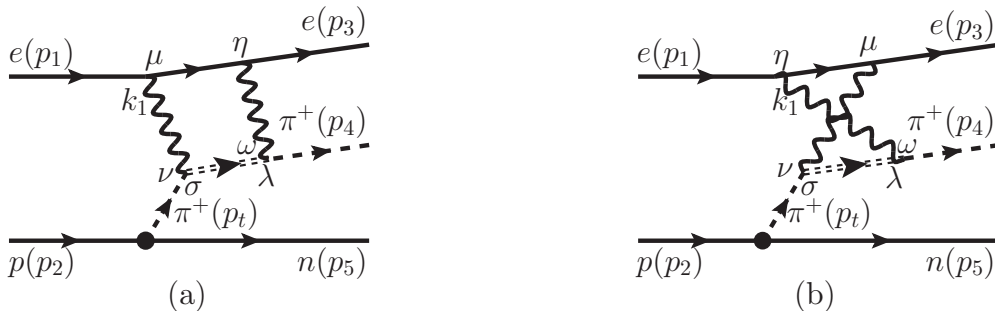


FIG. 8. Diagrams for $ep \rightarrow e\pi^+$ with two-photon exchange and one ρ meson intermediate state: (a) is the box diagram, and (b) is the crossed-box diagram.

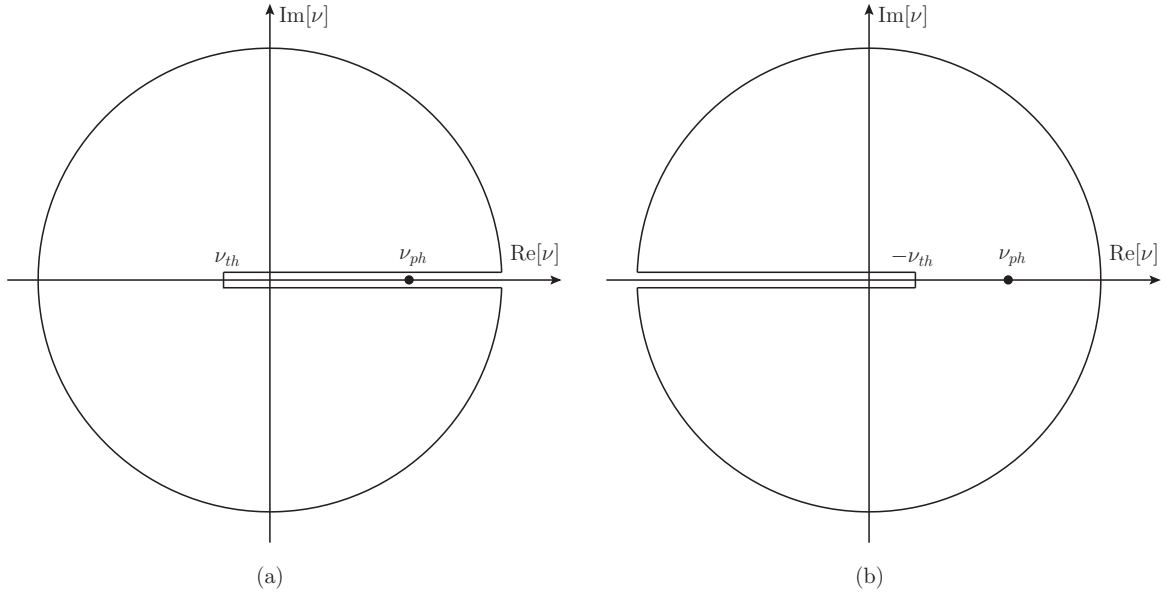


FIG. 9. The branch cuts of $c_{1,\pi;1,\rho}^{(a,b)}(\nu, Q^2, t)$ on the complex plane of ν at fixed physical Q^2 and t . (a) is for $c_{1,\pi;1,\rho}^{1,(a)}(\nu, Q^2, t)$ and (b) is for $c_{1,\pi;1,\rho}^{(b)}(\nu, Q^2, t)$ where $\nu_{\text{th}}^{(\pi)} = m_\pi^2 + 4m_e m_\pi - Q^2 - t$, $\nu_{\text{th}}^{(\rho)} = 2m_\rho^2 - m_\pi^2 + 4m_e m_\rho - Q^2 - t$, and ν_{ph} is the minimum physical ν .

The manifest expressions for $\text{Im}[c_{1,\pi;1,\rho}^{1,(a)}(\nu^+, Q^2, t)]$ are written as

$$\begin{aligned} & \text{Im}[c_{1,\pi}^{1,(a)}(\nu^+, Q^2, t)]|_{m_e \rightarrow 0} \\ &= \frac{2\pi\alpha_e^2}{Q^2(m_\pi^2 - t)} \theta(x_1 - 4m_e m_\pi) \\ & \times \left[\frac{1}{\tilde{\epsilon}_{\text{IR}}} + \ln \frac{4m_e^2(m_\pi^2 - t)^2 \bar{\mu}_{\text{IR}}^2}{x_1^2 Q^4} \right. \\ & \left. + \frac{2x_2}{x_2 Q^2 + y_1} \ln \frac{2x_2 Q^2}{x_1 x_3} \right], \end{aligned} \quad (14)$$

and

$$\begin{aligned} & \text{Im}[c_{1,\rho}^{1,(a)}(\nu^+, Q^2, t)]|_{m_e \rightarrow 0} \\ &= \frac{\pi\alpha_e^2 g_{\gamma\pi\rho}^2}{m_\rho^2(m_\pi^2 - t)} \theta(x_4 - 4m_e m_\pi) \\ & \times \left[\frac{x_4[3x_1 x_2 x_3 - 2m_\rho^2(2x_1 x_2 + 2x_2 x_3 - x_1 x_3)]}{8x_1 x_2^2 x_3} \right. \\ & \left. - \frac{x_2(\nu - 2m_\rho^2) + 2m_\pi^2 t + 2m_\rho^4}{2(x_2 Q^2 + y_1)} \ln \frac{2x_2 Q^2}{x_1 x_3} \right], \end{aligned} \quad (15)$$

with

$$\begin{aligned} x_1 &= Q^2 + t + \nu - m_\pi^2, \\ x_2 &= Q^2 + t + \nu + m_\pi^2, \\ x_3 &= Q^2 - t + \nu + m_\pi^2, \\ x_4 &= x_2 - 2m_\rho^2, \\ y_1 &= m_\pi^4 + m_\pi^2(Q^2 - 2t) + (t - \nu)(Q^2 + t + \nu). \end{aligned} \quad (16)$$

By the expressions of these imaginary parts and the DR, one can easily reproduce the real parts of $c_{1,\pi;1,\rho}^{1,(a+b)}(\nu, Q^2, t)$ via the numerical integration.

We want to emphasize a general property that $\text{Im}[c_{1,\pi}^{(a)}(\nu^+, Q^2, t)]$ has IR divergence and is dependent on the IR scale $\bar{\mu}_{\text{IR}}$. This is natural since the DR Eq. (13) means that $\text{Re}[c_{1,\pi}^{(a+b)}(\nu, Q^2, t)]$ is totally determined by $\text{Im}[c_{1,\pi}^{(a)}(\nu^+, Q^2, t)]$ and the former has IR divergence. The IR divergence in $\text{Re}[c_{1,\pi}^{(a+b)}(\nu, Q^2, t)]$ is canceled with that from the real radiative correction only at the cross-section level. This property hints that $\text{Im}[c_{1,\pi}^{(a)}(\nu^+, Q^2, t)]$ itself is not a physical observable. This is very different from the case in the forward angle limit where the imaginary part is corresponding to the physical total inclusive cross section via optical theorem. Some detailed discussion on the IR divergence of $\text{Re}[c_{1,\pi}^{(a+b)}(\nu, Q^2, t)]$ can be found in Ref. [19].

C. TPE contributions with EM FFs

Physically, the EM FFs $F_{\gamma\pi\pi}$ and $F_{\gamma\pi\rho}$ are not constants and the momentum dependence of the EM FFs should be considered when Q^2 increases. In the practical calculation, for simplicity the following monopole form FF is used [20,25].

$$F_{\gamma\pi\pi}^{\text{II}}(q^2) = F_{\gamma\pi\rho}^{\text{II}}(q^2) = \frac{-\Lambda^2}{q^2 - \Lambda^2}. \quad (17)$$

After the loop integration with this FF as inputs, we find the properties on the kinematic poles and the branch cuts of $c_{1,\pi;1,\rho}^{\text{II},(a,b)}$ are the same with those of $c_{1,\pi;1,\rho}^{1,(a,b)}$. The asymptotic

behaviors of $c_{1,\pi;1,\rho}^{\text{II},(a)}$ are expressed as follows:

$$\begin{aligned} & \text{Re}[c_{1,\pi}^{\text{II},(a)}(v^+, Q^2, t)] \\ & \xrightarrow{v \rightarrow \infty} \frac{2\alpha_e^2}{Q^2(m_\pi^2 - t)} \left[\frac{\Lambda^2}{\Lambda^2 + Q^2} \ln^2 v + a_{1,\pi}^{\text{II}} \ln v + O(v^0) \right], \\ & \text{Im}[c_{1,\pi}^{\text{II},(a)}(v^+, Q^2, t)] \\ & \xrightarrow{v \rightarrow \infty} \frac{2\pi\alpha_e^2}{Q^2(m_\pi^2 - t)} \left[\frac{-2\Lambda^2}{\Lambda^2 + Q^2} \ln v - a_{1,\pi}^{\text{II}} + O(v^{-1}) \right], \end{aligned} \quad (18)$$

and

$$\begin{aligned} & \text{Re}[c_{1,\rho}^{\text{II},(a)}(v^+, Q^2, t)] \xrightarrow{v \rightarrow \infty} a_{1,\rho}^{\text{II}} \ln v + O(v^0), \\ & \text{Im}[c_{1,\rho}^{\text{II},(a)}(v^+, Q^2, t)] \xrightarrow{v \rightarrow \infty} -2\pi a_{1,\rho}^{\text{II}} + O(v^{-1}), \end{aligned} \quad (19)$$

where $a_{1,\pi;1,\rho}^{\text{II}}$ are functions only dependent on m_π , m_ρ , t , Q^2 , and Λ .

Comparing the asymptotic behaviors Eqs. (19) and (20) and Eqs. (12) and (13), one can find an interesting property: the asymptotic behavior of $c_{1,\pi}^{\text{II},(a)}(v^+, Q^2, t)$ is similar with $c_{1,\pi}^{\text{I},(a)}(v^+, Q^2, t)$, but the asymptotic behavior of $c_{1,\rho}^{\text{II},(a)}(v^+, Q^2, t)$ is a little different from $c_{1,\rho}^{\text{I},(a)}(v^+, Q^2, t)$. The asymptotic behavior of $\text{Im}[c_{1,\pi}^{\text{I},(a)}(v^+, Q^2, t)]/\text{Im}[c_{1,\rho}^{\text{I},(a)}(v^+, Q^2, t)]$ is ~ 1 whereas $\text{Im}[c_{1,\pi}^{\text{II},(a)}(v^+, Q^2, t)]/\text{Im}[c_{1,\rho}^{\text{II},(a)}(v^+, Q^2, t)]$ is $\sim \ln v$. This property directly means that when v increases, the contributions with one ρ intermediate state are suppressed by a factor of $\ln v$ in the monopole FF case, whereas there is no such factor in the pointlike case.

The above properties also show that the TPE contribution $c_{1,\pi;1,\rho}^{\text{II},(a+b)}(v, Q^2, t)$ still satisfies the DR Eq. (13) when $m_e \rightarrow 0$. Practically, if one knows the analytic expressions of the imaginary parts, then one can easily get the real parts via Eq. (13) by the numerical integration. Since the analytic expressions of the imaginary parts can be used directly and conveniently via Eq. (13) by other groups to analyze the further experimental data or for comparison, we list the expressions for the imaginary parts in the following in the limit $m_e \rightarrow 0$.

The TPE contribution $c_{1,\pi}^{\text{II},(a)}(v, Q^2, t)$ includes IR divergence at first we separate it into two parts as

$$c_{1,\pi}^{\text{II},(a)}(v, Q^2, t) \equiv c_{1,\pi;\text{IR}}^{\text{II},(a)}(v, Q^2, t) + c_{1,\pi;\text{fin}}^{\text{II},(a)}(v, Q^2, t), \quad (20)$$

where $c_{1,\pi;\text{IR}}^{\text{II},(a)}(v, Q^2, t)$ only includes the term proportional to $\frac{1}{\epsilon_{\text{IR}}}$ and $c_{1,\pi;\text{fin}}^{\text{II},(a)}(v, Q^2, t)$ is the remaining part. We want to mention that the separation scheme is not unique. Here we just choose a scheme with a simple analytic form.

After the separation, the imaginary parts of the TPE contributions from one π , one ρ intermediate state are expressed

as follows:

$$\begin{aligned} & \text{Im}[c_{1,\pi;\text{IR}}^{\text{II},(a)}(v, Q^2, t)]|_{m_e \rightarrow 0} \\ & = \frac{2\pi\alpha_e^2}{Q^2(m_\pi^2 - t)} \theta(x_1 - 4m_e m_\pi) \frac{\Lambda^2}{\Lambda^2 + Q^2} \frac{1}{\tilde{\epsilon}_{\text{IR}}}, \\ & \text{Im}[c_{1,\pi;\text{fin}}^{\text{II},(a)}(v, Q^2, t)]|_{m_e \rightarrow 0} \\ & = \frac{2\pi\alpha_e^2}{Q^2(m_\pi^2 - t)} \theta(x_1 - 4m_e m_\pi) \sum_{i=1}^5 g_{\pi,i} \ln z_{\pi,i}, \\ & \text{Im}[c_{1,\rho}^{\text{II},(a)}(v, Q^2, t)]|_{m_e \rightarrow 0} \\ & = \frac{2\pi\alpha_e^2 g_{\gamma\pi\rho}^2}{m_\rho^2(m_\pi^2 - t)(y_1 + Q^2 x_2)} \theta(x_4 - 4m_e m_\pi) \sum_{i=1}^5 g_{\rho,i} \ln z_{\rho,i}, \end{aligned} \quad (21)$$

where

$$\begin{aligned} g_{\pi,1} & = \frac{\Lambda^2}{\Lambda^2 + Q^2}, \\ g_{\pi,2} & = \frac{\Lambda^2 x_3}{Q^2 x_1 + \Lambda^2 x_3}, \\ g_{\pi,3} & = \frac{Q^2(\Lambda^2 x_2 - y_1)}{(\Lambda^2 + Q^2)(Q^2 x_2 + y_1)}, \\ g_{\pi,4} & = \frac{Q^2(x_1 y_1 - \Lambda^2 x_2 x_3)}{(Q^2 x_2 + y_1)(Q^2 x_1 + \Lambda^2 x_3)}, \\ g_{\pi,5} & = \frac{Q^2[2\Lambda^2 x_2(Q^2 + v) - x_1 y_1]}{(Q^2 x_2 + y_1) y_2}, \\ z_{\pi,1} & = \frac{2\tilde{\mu}_{\text{IR}}^2 x_2}{x_1^2}, \\ z_{\pi,2} & = \frac{2m_e^2(m_\pi^2 - t)^2}{Q^4 x_2}, \\ z_{\pi,3} & = \frac{\Lambda^2(2\Lambda^2 x_2 + x_1 x_3)}{2x_2(\Lambda^2 + Q^2)^2}, \\ z_{\pi,4} & = \frac{x_1^2(Q^2 x_1 + \Lambda^2 x_3)^2}{2\Lambda^2 Q^4 x_2(x_1^2 + 2\Lambda^2 x_2)}, \\ z_{\pi,5} & = \frac{h_1 + x_1 y_2}{h_1 - x_1 y_2}, \\ g_{\rho,1} & = -\frac{1}{4}\Lambda^2 m_\rho^2, \\ g_{\rho,2} & = \frac{1}{8}(y_3 - m_\pi^2 x_5), \\ g_{\rho,3} & = -\frac{1}{8}(y_3 - m_\pi^2 x_5 + 2\Lambda^2 m_\rho^2), \\ g_{\rho,4} & = \frac{1}{4}\Lambda^2(m_\rho^2 - \Lambda^2), \\ g_{\rho,5} & = \frac{1}{8y_4} [Q^2 x_4(y_3 - m_\pi^2 x_5) + \Lambda^2(h_2 + m_\pi^2 y_5) \\ & \quad + 2\Lambda^4 y_6 - 4\Lambda^6(Q^2 + v)], \end{aligned} \quad (22)$$

and

$$\begin{aligned}
 z_{\rho,1} &= \frac{64x_2^2(m_\rho^2 - m_\pi^2)^2(m_\rho^2 - t)^2}{x_1^2x_3^2x_4^2}, \\
 z_{\rho,2} &= \frac{Q^4x_4^2}{16(m_\rho^2 - m_\pi^2)^2(m_\rho^2 - t)^2}, \\
 z_{\rho,3} &= \frac{x_4^2(Q^2x_4 + \Lambda^2x_1)^2(Q^2x_4 + \Lambda^2x_3)^2}{16\Lambda^4(m_\rho^2 - m_\pi^2)^2(m_\rho^2 - t)^2\{x_1x_3x_4^2 + 4\Lambda^2x_2[x_4(Q^2 + \nu) + \Lambda^2x_2]\}}, \\
 z_{\rho,4} &= \frac{4\Lambda^4x_2^2}{x_1x_3x_4^2 + 4\Lambda^2x_2[x_4(Q^2 + \nu) + \Lambda^2x_2]}, \\
 z_{\rho,5} &= \frac{x_4(Q^2x_4 + y_4) + 2\Lambda^2x_4(Q^2 + \nu) + 4\Lambda^4x_2}{x_4(Q^2x_4 - y_4) + 2\Lambda^2x_4(Q^2 + \nu) + 4\Lambda^4x_2},
 \end{aligned} \tag{25}$$

with

$$\begin{aligned}
 x_5 &= \nu + t - 2m_\rho^2, \\
 y_2 &= \sqrt{4\Lambda^4[m_\pi^4 + 2m_\pi^2(Q^2 - t) + 2Q^4 + 2Q^2(t + \nu) + t^2] + 4\Lambda^2Q^2(Q^2 + \nu)x_1 + Q^4x_1^2}, \\
 y_3 &= -2m_\rho^4 + (2m_\rho^2 - \nu)(Q^2 + t + \nu), \\
 y_4 &= \sqrt{4\Lambda^4[m_\pi^4 + 2m_\pi^2(Q^2 - t) + 2Q^4 + 2Q^2(t + \nu) + t^2] + 4\Lambda^2Q^2(Q^2 + \nu)x_4 + Q^4x_4^2}, \\
 y_5 &= 4m_\rho^2(2Q^2 + \nu) - 2(Q^2 + \nu)(2t + \nu), \\
 y_6 &= 2m_\pi^4 + m_\pi^2(3Q^2 - 4t) + 2m_\rho^2(3Q^2 + 2\nu) + (Q^2 + 2t - 2\nu)(Q^2 + t + \nu), \\
 h_1 &= 4\Lambda^4x_2 + 2\Lambda^2(Q^2 + \nu)x_1 + Q^2x_1^2, \\
 h_2 &= -4m_\rho^4(3Q^2 + \nu) + 4m_\rho^2(2Q^2 + \nu)(Q^2 + t + \nu) - 2\nu(Q^2 + \nu)(Q^2 + t + \nu).
 \end{aligned} \tag{26}$$

Practically, by submitting Eq. (20) into Eq. (13) and performing the numerical integration, one can easily get the full TPE contributions at any kinematic region using a few lines of codes in *Mathematica*. These numerical results can be directly used in the analyses of the experimental data sets or for comparison.

We also want to point out that the contributions $c_{2,\pi;2,\rho}^{\text{II},(a+b)}$ are nonzero and do not satisfy the DR Eq. (13) when m_e is taken as nonzero, whereas that is another topic.

To get the final finite and IR scale-independent correction, one should subtract $c_{1,\pi}^{\text{II},(a+b)}$ by the soft contribution which is used in the experimental data analysis. The practical calculation shows that the finite part $c_{1,\pi;\text{fin}}^{\text{II},(a+b)}$ with $\bar{\mu}_{\text{IR}} = 1$ GeV is very close to the corresponding finite result which subtracts the classical IR result by Mo and Tasi [26] from the full result. The choice of $\bar{\mu}_{\text{IR}} = 1$ GeV is equivalent to choose $\lambda = 1$ GeV in the mass regularization where λ is the infinitesimal mass of the photon. Due to these

properties and the fact that Mo and Tsai's [26] IR is usually used, we take $\bar{\mu}_{\text{IR}} = 1$ GeV directly in the finite part in the following.

IV. THE NUMERICAL RESULTS FOR $c_{1,\pi;1,\rho}^{\text{II},(a+b)}/c_1^{(1\gamma)}$

Usually, the experimental quantities Q^2 , W , ϵ , θ_π , and ϕ_π are chosen as variables to express the differential cross section where ϵ is the virtual photon polarization, θ_π and ϕ_π are the angles between the three-momentum of π and the ep -scattering plane. Their detailed definitions can be found in the Appendix of Ref. [19]. In the point-dominance approximation as discussed above the coefficients of the invariant amplitudes are only dependent on ν , t , and Q^2 when taking Q^2 , W , ν , t , and s as five independent variables. This property means it is much simpler to show the TPE contributions by choosing the latter quantities as independent variables. In the following, at first we present the numeric results with the latter choice,

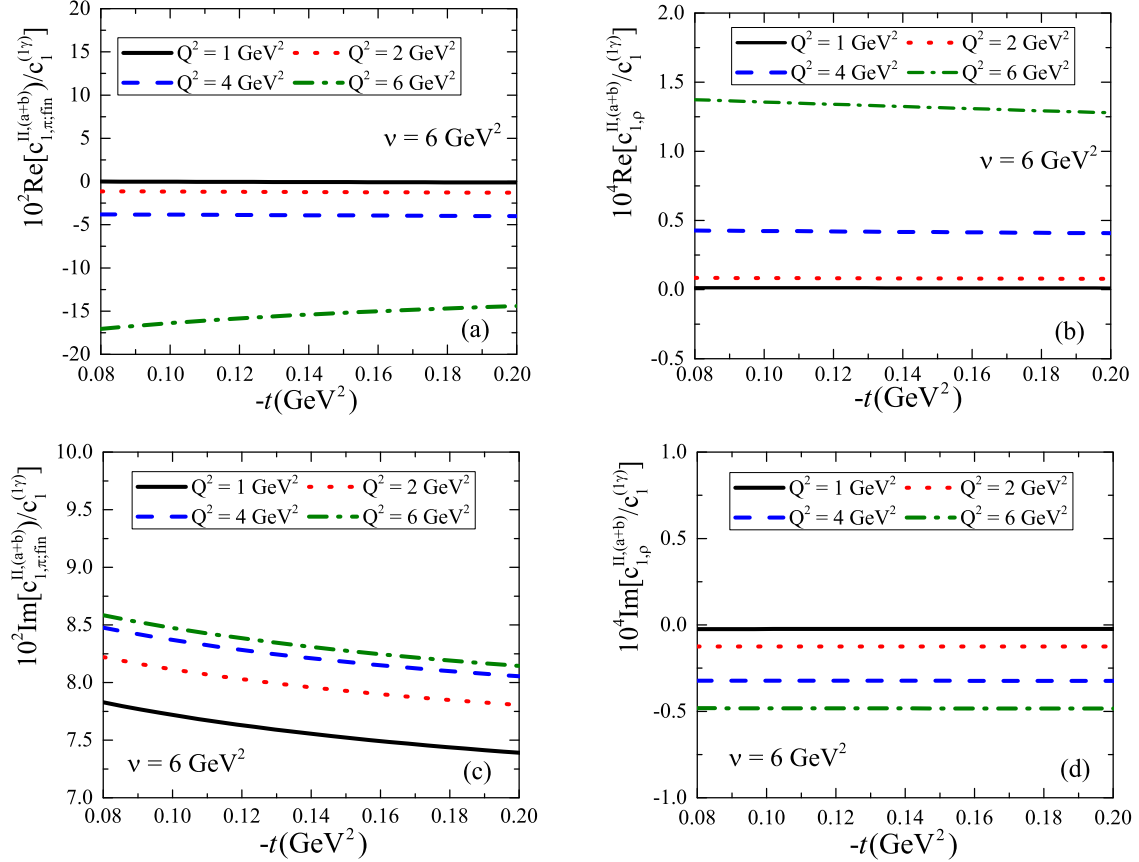


FIG. 10. Numeric results for $c_{1,\pi;\text{fin}}^{\text{II},(a+b)}/c_1^{(1\gamma)}$ vs $-t$ and $c_{1,\rho}^{\text{II},(a+b)}/c_1^{(1\gamma)}$ vs $-t$ at fixed Q^2 , ν . The top panel is for the real part, and the bottom panel is for the imaginary part.

and then present the numeric results with the experimental variables as inputs.

In Fig. 10, the numeric results for $c_{1,\pi;\text{fin}}^{\text{II},(a+b)}/c_1^{(1\gamma)}$ and $c_{1,\rho}^{\text{II},(a+b)}/c_1^{(1\gamma)}$ are presented at $Q^2 = 1, 2, 4, 6 \text{ GeV}^2$ with $\nu = 6 \text{ GeV}^2$. Here we have taken the IR scale as $\bar{\mu}_{\text{IR}} = 1 \text{ GeV}$, the parameter in the FFs as $\Lambda = 0.77 \text{ GeV}$, and the coupling constant as $g_{\gamma\pi\rho} = 0.103$ which is determined by the decay width of $\rho^+ \rightarrow \gamma\pi^+$. The numeric results clearly show that the TPE contributions with one ρ meson intermediate state are much smaller than those with one π intermediate state in the chosen regions. This interesting property is very different from the property in the elastic ep -scattering case where the contributions from the inelastic intermediate states are at the same order with those from an elastic intermediate state. The numeric results also show that the absolute magnitudes of the TPE corrections increase when Q^2 increases. When $\nu = 6 \text{ GeV}^2$, the magnitudes of $\text{Re}[c_{1,\pi;\text{fin}}^{\text{II},(a+b)}/c_1^{(1\gamma)}]$ and $\text{Re}[c_{1,\rho}^{\text{II},(a+b)}/c_1^{(1\gamma)}]$ are about 15% and 0.15% at $Q^2 = 6 \text{ GeV}^2$ and about 4% and 0.005% at $Q^2 = 4 \text{ GeV}^2$, respectively. Another very interesting property is that the TPE corrections are not sensitive on the variable t when ν and Q^2 are fixed.

In Fig. 11, we take the kinematics in the F_π experiment of the JLab Collaboration [15] with $Q^2 = 1, 1.6 \text{ GeV}^2$ at $W = 1.95 \text{ GeV}$ as examples to show the numerical results for $\text{Re}[c_{1,\pi;\text{fin}}^{\text{II},(a+b)}/c_1^{(1\gamma)}]$ and $\text{Re}[c_{1,\rho}^{\text{II},(a+b)}/c_1^{(1\gamma)}]$.

The numerical results for $\text{Re}[c_{1,\pi;\text{fin}}^{\text{II},(a+b)}/c_1^{(1\gamma)}]$ are the same as those in Ref. [19] where they are labeled as $\text{Re}[c_{1,\pi;\text{fin}}^{(2\gamma)}/c_1^{(1\gamma)}]$. The (blue) dashed curves and the (olive) dashed-dot curves refer to the results at $\phi_\pi = \pi/6$ and $\phi_\pi = \pi/3$ with $\epsilon = 0.65$ or 0.63 , and the (black) solid curves and the (red) dotted curves are associated with $\epsilon = 0.33$ or 0.27 . The results clearly show that the absolute magnitude of TPE corrections $\text{Re}[c_{1,\rho}^{\text{II},(a+b)}/c_1^{(1\gamma)}]$ are smaller than 10^{-4} at $Q^2 = 1 \text{ GeV}^2$ and smaller than 10^{-3} at $Q^2 = 1.6 \text{ GeV}^2$. These corrections are much smaller than the results with one π meson intermediate state [19]. In the practical estimation, one can use Eqs. (13) and (22) to get $\text{Re}[c_{1,\pi;\text{fin}}^{\text{II},(a+b)}/c_1^{(1\gamma)}]$ easily and then check this property in other regions. This property suggests that the TPE corrections with one ρ meson intermediate state can be relatively negligible in the current experimental regions.

To summarize in this paper the TPE contributions in $ep \rightarrow e\pi^+$ with one π and one ρ intermediate state are estimated under the pion-dominance approximation within the hadronic model. The calculation shows that these TPE contributions satisfy an un-subtracted DR when $m_e \rightarrow 0$. The analytic expressions for the imaginary parts of the TPE contributions within the hadronic model are given. Combine these analytic expressions and the DR, one can get the real parts of the TPE contributions at any available kinematic region easily. We think these expression can help the further experimental

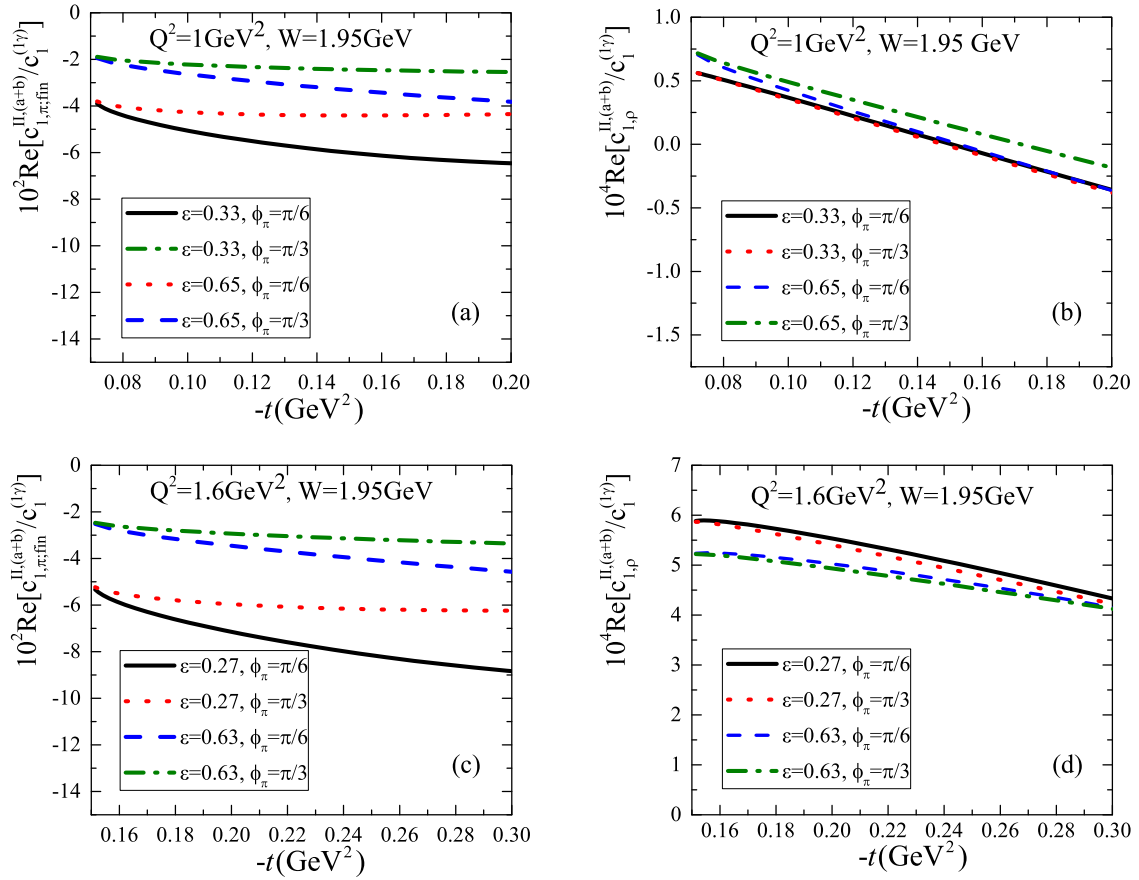


FIG. 11. Numeric results for $\text{Re}[c_{1,\pi,\text{fin}}^{II(a+b)}/c_1^{(1\gamma)}]$ vs. $-t$ and $\text{Re}[c_{1,\rho}^{II(a+b)}/c_1^{(1\gamma)}]$ vs. $-t$ at fixed Q^2 , W , ϵ , and ϕ_π .

analysis to include the TPE contributions conveniently. On the numerical part, we find the contributions from one ρ intermediate state are much smaller than those from one π intermediate state. This suggests that the estimation only with one π intermediate state can be applied to higher Q^2 and higher ν safely.

ACKNOWLEDGMENTS

H.-Q.Z. thanks H. Patel for his kind help with PACKAGE-X. This work was supported by the National Natural Science Foundations of China under Grants No. 12075058 and No. 11975075.

- [1] P. G. Blunden, W. Melnitchouk, and J. A. Tjon, *Phys. Rev. Lett.* **91**, 142304 (2003); S. Kondratyuk, P. G. Blunden, W. Melnitchouk, and J. A. Tjon, *ibid.* **95**, 172503 (2005); P. G. Blunden, W. Melnitchouk, and J. A. Tjon, *Phys. Rev. C* **72**, 034612 (2005).
- [2] Y. C. Chen, A. Afanasev, S. J. Brodsky, C. E. Carlson, and M. Vanderhaeghen, *Phys. Rev. Lett.* **93**, 122301 (2004); A. V. Afanasev, S. J. Brodsky, C. E. Carlson, Y.-C. Chen, and M. Vanderhaeghen, *Phys. Rev. D* **72**, 013008 (2005).
- [3] N. Kivel and M. Vanderhaeghen, *Phys. Rev. Lett.* **103**, 092004 (2009); V. N. Pomerantsev, V. I. Kukuln, and O. A. Rubtsova, *Phys. Rev. C* **79**, 034001 (2009).
- [4] D. Borisyuk and A. Kobushkin, *Phys. Rev. C* **74**, 065203 (2006); **83**, 025203 (2011); **86**, 055204 (2012); **89**, 025204 (2014).
- [5] O. Tomalak and M. Vanderhaeghen, *Eur. Phys. J. A* **51**, 24 (2015); P. G. Blunden and W. Melnitchouk, *Phys. Rev. C* **95**, 065209 (2017); O. Tomalak, B. Pasquini, and M. Vanderhaeghen, *Phys. Rev. D* **96**, 096001 (2017).
- [6] N. Kivel and M. Vanderhaeghen, *J. High Energy Phys.* **04** (2013) 029.
- [7] P. Talukdar, V. C. Shastry, U. Raha, and F. Myhrer, *Phys. Rev. D* **101**, 013008 (2020); **104**, 053001 (2021); X.-H. Cao, Q.-Z. Li, and H.-Q. Zheng, *ibid.* **105**, 094008 (2022).
- [8] Y. C. Chen, C. W. Kao, and S. N. Yang, *Phys. Lett. B* **652**, 269 (2007); D. Borisyuk and A. Kobushkin, *Phys. Rev. C* **76**, 022201 (2007).
- [9] A. V. Gramolin *et al.*, *Nucl. Phys. B, Proc. Suppl.* **225-227**, 216 (2012).
- [10] D. M. Nikolenko *et al.*, *EPJ Web Conf.* **66**, 06002 (2014).
- [11] M. Moteabbed *et al.* (CLAS Collaboration), *Phys. Rev. C* **88**, 025210 (2013).
- [12] M. Kohl *et al.* (OLYMPUS Collaboration), *EPJ Web Conf.* **66**, 06009 (2014).
- [13] C. J. Bebek *et al.*, *Phys. Rev. D* **13**, 25 (1976); C. J. Bebek, C. N. Brown, S. D. Holmes, R. V. Kline, F. M. Pipkin, S. Raither, L. K. Sistierson, A. Browman, K. M. Hanson, D. Larson, and A. Silverman, *ibid.* **17**, 1693 (1978).

- [14] P. Brauel *et al.* (DESY Collaboration), *Phys. Lett. B* **65**, 184 (1976); **69**, 253 (1977); H. Ackermann *et al.*, *Nucl. Phys. B* **137**, 294 (1978); P. Brauel *et al.*, *Z. Phys. C: Part. Fields* **3**, 101 (1979).
- [15] J. Volmer *et al.* (Jefferson Lab $F\pi$ Collaboration), *Phys. Rev. Lett.* **86**, 1713 (2001); T. Horn *et al.* (Jefferson Lab $F\pi$ Collaboration), *ibid.* **97**, 192001 (2006); V. Tadevosyan *et al.* (Jefferson Lab $F\pi$ Collaboration), *Phys. Rev. C* **75**, 055205 (2007).
- [16] H. P. Blok, T. Horn *et al.* (Jefferson Lab $F\pi$ Collaboration), *Phys. Rev. C* **78**, 045202 (2008).
- [17] G. M. Huber *et al.* (Jefferson Lab $F\pi$ Collaboration), *Phys. Rev. C* **78**, 045203 (2008).
- [18] A. Afanasev, A. Aleksejevs, and S. Barkanova, *Phys. Rev. C* **88**, 053008 (2013).
- [19] H. Y. Cao and H. Q. Zhou, *Phys. Rev. C* **101**, 055201 (2020).
- [20] H. Q. Zhou, *Phys. Lett. B* **706**, 82 (2011).
- [21] T. Feuster and U. Mosel, *Phys. Rev. C* **59**, 460 (1999).
- [22] R. Mertig, M. Bohm, and A. Denner, *Comput. Phys. Commun.* **64**, 345 (1991); V. Shtabovenko, R. Mertig, and F. Orellana, *ibid.* **207**, 432 (2016).
- [23] H. H. Patel, *Comput. Phys. Commun.* **197**, 276 (2015); **218**, 66 (2017).
- [24] T. Hahn and M. Perez-Victoria, *Comput. Phys. Commun.* **118**, 153 (1999).
- [25] P. G. Blunden, W. Melnitchouk, and J. A. Tjon, *Phys. Rev. C* **81**, 018202 (2010).
- [26] L. W. Mo and Y. S. Tsai, *Rev. Mod. Phys.* **41**, 205 (1969); Y. S. Tsai, *Phys. Rev.* **122**, 1898 (1961).